Improvement in Instability of Transparent ALD ZnO TFTs under Negative Bias Illumination Stress with SiO_2/Al_2O_3 Bilayer Dielectric

Wanpeng Zhao, Ning Zhang, Xinyu Zhang, Chong Yao, Junfeng Zhang, Shurong Dong, *Senior Member, IEEE*, Yang Liu, Zhi Ye, *Member, IEEE*, and Jikui Luo

***Abstract*—The theory of oxygen vacancy related deep energy defects and valence band offset (VBO) between gate insulator and channel codetermining the threshold voltage shift (ΔV_{TH}) of ZnO thin film transistor under negative gate bias and illumination stress (NBIS) is proposed and investigated systematically. Two kinds of ZnO thin film transistors are fabricated by atomic layer deposition with different gate oxide structures, a control sample with Al_2O_3 gate oxide and an improved sample with SiO_2/Al_2O_3 gate oxide structures. Among two kinds of devices, the device with SiO_2/Al_2O_3 gate oxide achieves a smaller ΔV_{TH} under the NBIS with SiO_2 thin film acting as a holes-blocking layer, despite the existence of more defects than control device. The improvement in stability is attributed to large VBO up to 3.08 eV. Moreover, the device with SiO_2/Al_2O_3 gate oxide is evaluated on a 500-nit LCD back light to simulate the practical working environment in displays, which exhibits good stability of ΔV_{TH}= -0.3 V for 3600 seconds.**

***Index Terms*—Zinc oxide, thin-film transistor, negative bias illumination stress (NBIS), stability, holes-blocking layer (HBL).**

I. Introduction

In recent years, smartphones have pushed on a rapid development in advanced active matrix organic light emitting diodes (AMOLED) displays demanding high resolution and high refresh rate. To keep balance between long battery life and high power consumption resulting from high refresh rate, low temperature polycrystalline oxide (LTPO) is proposed as an emerging technology for next-generation displays, which combines the high mobility of the low temperature poly-silicon (LTPS) thin film transistors (TFTs) and the low leakage current of the metal oxide TFTs [1-3]. Especially, nano-crystalline zinc oxide (ZnO) is a representative material of channels in oxide TFTs that can be used in LTPO backplane for its high mobility, high ON/OFF ratio, low leakage current, good uniformity and high optical transparency [4]. Except for these advantages, ZnO TFTs like other oxide-based TFTs still suffer from some problems, such as the threshold voltage (V_{TH}) shift under gate bias and illumination stress[5, 6]. In our previous works [6-8], ZnO TFTs exhibit good reliability under negative and positive gate bias stress (NGBS, PGBS), but a great negative shift of V_{TH} under negative gate bias and illumination stress (NBIS). This phenomenon will cause failure of display when TFTs stay in off-state with negative gate voltage and light emitting from OLED, ambient illumination or sunlight, because the switching TFTs could be turned on improperly. Although various reports tried to explain this serious NBIS phenomenon, including injection of photo-excited holes into the gate dielectric or the interface of channel and gate insulator [9-11], valence band offset [12], ionization of oxygen vacancy [13, 14], subgap states attributed to oxygen vacancy defects [15-17] and ambient atmosphere [18, 19], the mechanisms of NBIS in oxide TFTs are still ambiguous and even contradictory due to the different device structures and materials. The origin of the NBIS in oxide TFTs is usually complex and induced by various factors concurrently.

This work was supported in part by the NSFC under Grant 61501401 and Grant 61774132, in part by the National Science Foundation of Zhejiang Province, China, under Grant LZ20F040003 and Grant LD22E030007, in part by Sichuan Science and Technology Agency, under Grant 2019YFSY0043. *(Corresponding author: Zhi Ye, Jikui Luo)*

Wanpeng Zhao, Ning Zhang, Xinyu Zhang, Chong Yao, Junfeng Zhang, Shurong Dong, Yang Liu, Zhi Ye, and Jikui Luo are with the College of Information Science & Electronic Engineering, Zhejiang University, Hangzhou 310027, China and International Joint Innovation Center, Zhejiang University, Haining 314400, China (e-mail: yezhi@zju.edu.cn, jackluo@zju.edu.cn).

Meanwhile, many methods were proposed to solve the instability of the oxide-based TFTs, for example, versatile light shielding design [20, 21], change of the defect and band state by reactive oxygen radicals [22], using a distributed bragg reflectors composed of ZnS and LiF as functional passivation layers [23], passivating defects in oxide semiconductors with fluorination, oxidation and boron addition [13, 24-30], passivation layers [31], and so on. Therefore, clarifying the origin of instability of V_{TH} induced by NBIS and developing a valid approach to suppress this issue without extra complicated treatment and cost are extremely important for application of oxide-based TFTs in current and future transparent displays.

In this article, two-type devices with different dielectric structure designs are fabricated and evaluated under NGBS with white LED, different wavelengths laser of 405 nm ~ 650 nm. It is observed that the degradation of devices under NBIS attributes to the co-effect of deep energy donor-like defects and valence band offset (VBO). Eventually, the device with silicon oxide (SiO_2) /alumina (Al_2O_3) multi-layer gate oxide exhibits less ΔV_{TH} under NBIS than initial devices due to its large VBO. In actual working environment, the device achieves a good stability of ΔV_{TH}= -0.3 V under NBIS.

II. Experiments

The structures of two devices with different designs of gate insulator are illustrated in Fig. 1(a) and Fig. 1(b) respectively. The source/drain electrodes of indium-tin-oxide (ITO) (200 nm) were deposited by DC magnetron sputtering and patterned in aqua regia on a glass substrate at first. Then a 20 nm thick ZnO layer was deposited by atomic layer deposition (ALD) as channel. Subsequently, a 10 nm thick Al_2O_3 layer was deposited

This article has been accepted for publication in IEEE Journal of the Electron Devices Society. This is the author's version which has not been fully edited and content may change prior to final publication. Citation information: DOI 10.1109/JEDS.2022.3212477

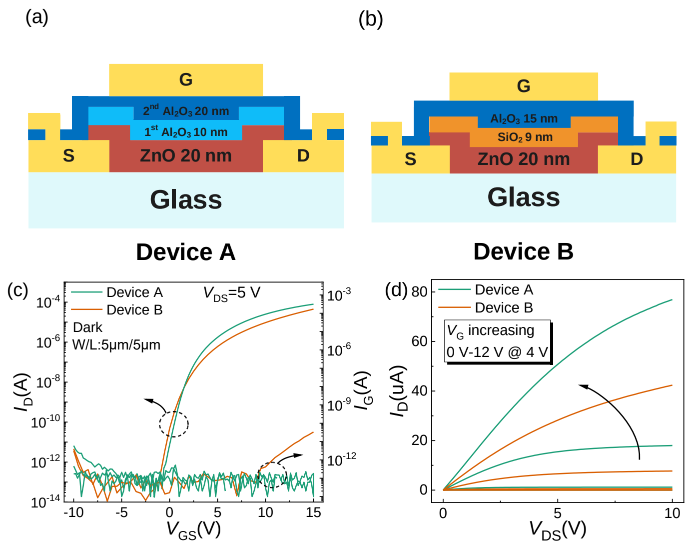

Fig. 1. Cross-sectional schematics of (a) Device A and (b) Device B. (c) Transfer characteristics and (d) output curves of device A and B.

TABLE I
ELECTRICAL PARAMETERS OF TWO-TYPE TFTS

Type	Device A	Device B
Dielectric	30 nm Al_2O_3	15 nm Al_2O_3
HBL*	N/A	9 nm SiO_2
W/L	5 μm/5 μm	5 μm/5 μm
C_{ox} (nF/cm^2)	186	197
μ_{FE} ($cm^2\ V^{-1}s^{-1}$)	17.9	11.36
V_{TH} (V)	3.23	2.56
I_{ON}/I_{OFF}	10^{10}	10^{10}
***SS* ($mV\cdot dec^{-1}$)**	225	271
N_{it} ($cm^{-1}e^{-1}V^{-1}$)	2.97×10^{12}	3.8×10^{12}

*: Holes blocking layer

by ALD as protection/gate oxide layer in device A and a 9 nm thick SiO_2 layer was deposited by RF magnetron sputtering as a holes-blocking layer (HBL) in device B. The second gate insulator of device A/B were a 20 nm thick Al_2O_3 layer and a 15 nm thick Al_2O_3 layer, respectively. The Al_2O_3 film was prepared by thermal ALD at 200 °C using trimethylaluminum (TMA) and water as precursor and oxidant respectively. A 100 nm thick ITO layer was deposited by DC magnetron sputtering and patterned as gate electrode by lift-off process. Finally, these devices were annealed at 400 °C in O_2 for 5 minutes. The devices were tested under NBIS with different light sources: white LED of 1200 lux, red laser (650 nm) of 57000 lux, green laser (532 nm) of 311400 lux, cyan laser (488 nm) of 3400 lux, blue laser (450 nm) of 6500 lux, and purple laser (405 nm) of 650 lux.

The field-effect mobility (μ_{FE}), subthreshold swing (*SS*) and the charge trap density of interface between the channel and dielectric layers (N_{it}) are extracted by the following equations:

$$\mu_{FE} = \frac{\frac{dI_D}{dV_{GS}}}{C_{ox}\frac{W}{L}V_{DS}} \quad (1)$$

$$SS = \frac{dV_{GS}}{d(\log I_D)} \quad (2)$$

$$N_{\rm it} = \frac{C_{\rm ox}}{q}\left(\frac{qSS}{k_{\rm B}T\ln 10} - 1\right) \quad (3)$$

where *W* and *L* are the channel width and length, respectively; V_{GS}, V_{DS} and I_D represent gate voltage, drain voltage and drain current, respectively; C_{ox} means the capacitance per unit area

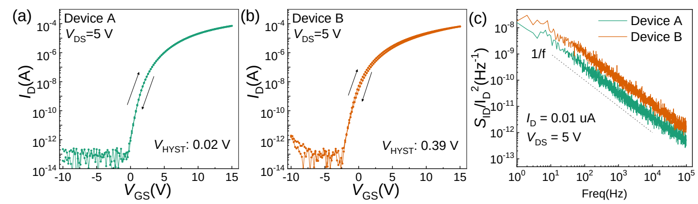

Fig. 2. Double sweep of transfer characteristics under V_D=5 V of (a) device A and (b) device B. (c) Normalized drain current noise spectral density of device A and B.

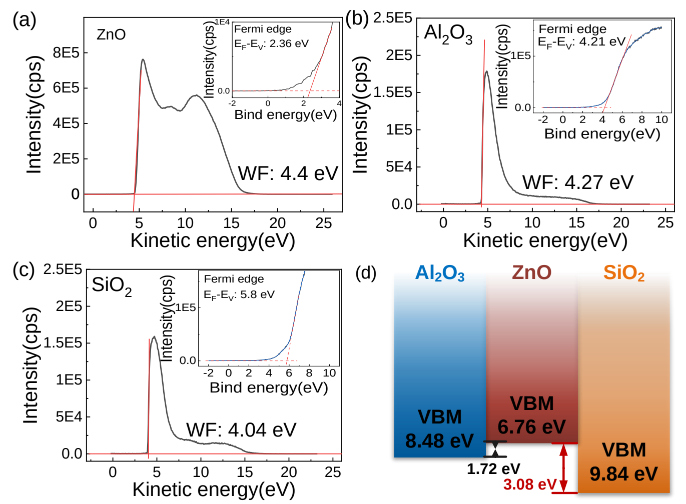

Fig. 3. UPS spectrum and its VB region (inset) of (a) ZnO, (b) Al_2O_3 and (c) SiO_2 to determine the value of work function and valence band maximum relative to fermi level by linear fit. (d) Valence band maximum's diagram of ZnO, Al_2O_3 and SiO_2.

of the insulator; q is the electron charge and $k_{\rm B}$ and T are the Boltzmann constants and the measurement temperature, respectively.

The electrical characteristics and energy band structures of these devices were measured respectively by semiconductor parameter analyzer (Agilent B1500A) and UPS (HeI: 21.22 eV, Kratos Axis Spura). The spectrum and illumination were measured by spectrograph (OHSP-350UV).

III. RESULTS AND DISCUSSION

Fig. 1(c) shows the I_D-V_G of the two types of devices, and their μ_{FE}, *SS* and N_{it} are extracted according to equations (1) (2) (3) listed in Table I. The results reveal that device A exhibits higher field-effect mobility of 17.9 cm^2/Vs, compared with device B of field-effect mobility of 11.36 cm^2/Vs at V_{DS} of 5 V. The I_{ON}/I_{OFF} ratios of device A/B are over 10^{10} due to the good quality dielectric layer of Al_2O_3. The *SS* values of device A/B are 225 mV/dec, 271 mV/dec respectively. Therefore, the N_{it} of device A and B can be estimated by equation (3) with values of 2.97×10^{12} $cm^{-2}e^{-1}V^{-1}$ and 3.80×10^{12} $cm^{-2}e^{-1}V^{-1}$ respectively [32], because of the bombardment of high-speed particles in magnetron sputtering of SiO_2 resulting in more interfacial defects at interface of SiO_2/ZnO. These defects also impede the movement of carriers and reduce the mobility of device B. The saturation current of device A is close to 80 μA, higher than that of device B as shown in Fig. 1(d), which also confirms conclusion above. Also, the double sweep of transfer characteristics of different ZnO TFTs were measured as shown in Fig. 2(a) and (b). Both devices exhibit clockwise hysteresis due to electrons trapped at the channel/insulator interface. Device B with HBL exhibits a large hysteresis of 0.39 V, while

This article has been accepted for publication in IEEE Journal of the Electron Devices Society. This is the author's version which has not been fully edited and content may change prior to final publication. Citation information: DOI 10.1109/JEDS.2022.3212477

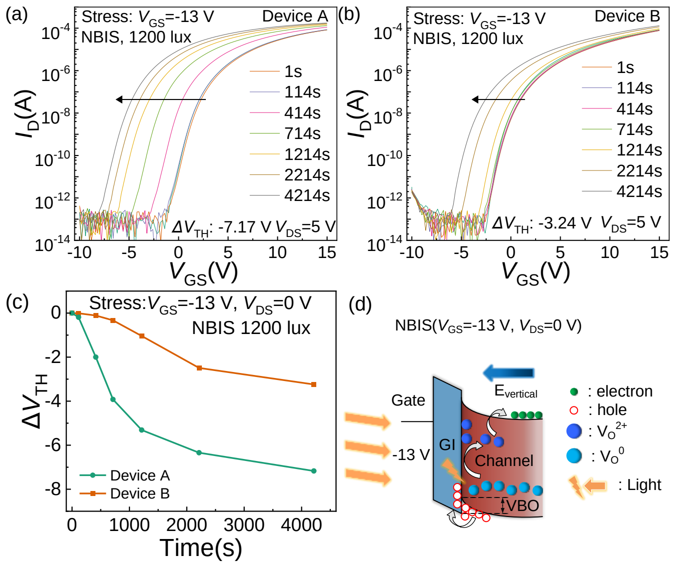

Fig. 4. The transfer characteristics of (a) device A and (b) device B at V_{GS}=-13 V, V_{DS}=0 V for 4214 s with white LED of 1200 lux. (c) The ΔV_{TH} of device A and device B at V_{GS}=-13 V, V_{DS}=0 V for 4214 s with white LED of 1200 lux. (d) The schematic mechanism diagram of the threshold voltage shifting under NBIS.

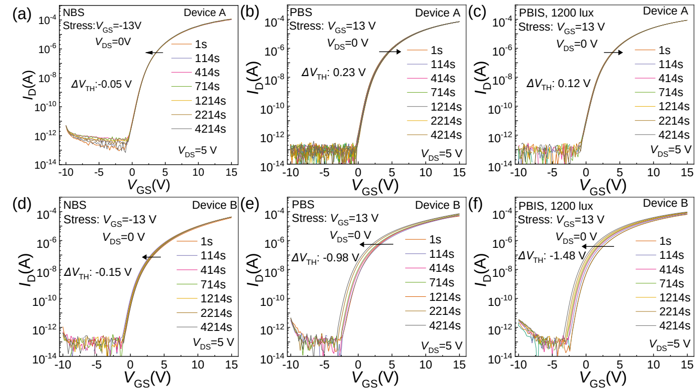

Fig. 5. The transfer curves of device A under (a) NBS of V_{GS}=-13 V, V_{DS}=0 V, (b) PBS of V_{GS}=13 V, V_{DS}=0 V, (c) PBIS of V_{GS}=13 V, V_{DS}=0 V with white LED of 1200 lux for 4214 s and the transfer curves of device B under the same condition of device A: (d) NBS (e) PBS (f) PBIS.

TABLE II
THRESHOLD VOLTAGE SHIFT OF TFTS UNDER VARIOUS STRESSES

Type \ ΔV_{TH}	NBIS	NBS	PBS	PBIS
Device A	-7.17 V	-0.05 V	0.23 V	0.12 V
Device B	-3.24 V	-0.15 V	-0.98 V	-1.48 V

device A shows a negligible hysteresis of 0.02 V. According to the formula $N_{it} \propto C_{OX}\Delta V_{TH}$ [33], SiO_2 thin film deposited by sputtering increases the interface trap density and reduces the mobility, which are consistent with *SS* values above. Furthermore, the normalized drain current noise spectral density of device A and device B is also measured to evaluate the defects as shown in Fig. 2(c). When device A/B achieve the same drain current of 0.01 μA, device B shows higher noise than device A in subthreshold regime attributed to larger subgap density of states (DOSs) at the interface of channel and insulator [34, 35]. Therefore, the RF magnetron sputtering of SiO_2 film results in more interface traps than atomic layer deposition of Al_2O_3 film. In addition, SiO_2 as single insulator in our top gate structure device would cause large gate leakage current and hysteresis [36]. Thus, a bilayer insulator of SiO_2/Al_2O_3 is chosen in device B to improve these performances.

To determine the VBO of ZnO and insulator fabricated in this experiment, the VBM of ZnO, Al_2O_3 and SiO_2 are measured by UPS. From Fig. 3(a), (b) and (c), the work function and the valence band maximum relative to fermi level (inset) can be extracted by linear fit, and the valence band maximum relative to vacuum level can be calculated as the sum of these values. Fig. 3(d) depicts that the practical VBM of ZnO, Al_2O_3 and SiO_2 are 6.76 eV, 8.48 eV and 9.84 eV, and the VBO of ZnO/Al_2O_3, ZnO/SiO_2 are 1.72 eV and 3.08 eV, respectively. Thus, device B shows higher VBO than device A.

Then, the stability of device A/B under NBIS is evaluated. The illumination is a white LED (1200 lux, 0.36 mW/cm^2) with wavelength ranging from 390 nm to 720 nm (1.72 eV to 3.18 eV). The transfer characteristics of device A and B under NBIS are shown in Fig. 4(a) and (b). Fig. 4(c) demonstrates the V_{TH} changes of devices under different duration of NBIS. Under negative stress of V_{GS}=-13 V with white LED of 1200 lux for 4214 s, device A and B exhibit the ΔV_{TH} of -7.17 V and -3.24 V, respectively. Obviously, device B achieves the lower ΔV_{TH} than device A, which means that the SiO_2 as HBL could prevent holes from being injected into the gate insulator effectively and significantly improve the NBIS induced instability.

The schematic energy band diagram in Fig. 4(d) explains the probable principle of threshold voltage shift under NBIS. For one thing, the holes accumulated in the valence band overcome the energy barrier of valence band offset (VBO) and jump into the gate insulator under the combined action of negative gate bias and illumination [12]. As mentioned above, the results of low N_{it} extracted from *SS* of the two devices demonstrate that device B has worse interface, while device B has better stability under NBIS. Therefore, the results of NBIS indeed reveal that widening VBO between the gate insulator and the active layer could suppress the threshold voltage shift of TFTs under NBIS. The higher energy barrier makes the holes excited by light to be injected into the gate insulator more difficult under negative bias. For another, HBL could not fully eliminate the instability induced by NBIS, since the donor-like defects in deep level also play important role in instability of TFTs. The donor-like defects are generally believed to be related to oxygen vacancies [15, 24, 27-30]. The V_O would be ionized and excited to be V_O^{2+} under illumination. The excited electrons jump to conduction band and are pushed out under the negative voltage. The ionized V_O^{2+} acted as fixed positive charge forms extra positive electric field applied on the channel. Therefore, the TFTs would be turned on early.

Furthermore, the reliability of device A/B under PBIS, PBS and NBS is evaluated. The transfer characteristics and summary are shown in Fig. 5 (a)-(f) and listed in Table II. Fig. 5(a) and (d) show that device A has negligible negative shift of V_{TH} under NBS for 4214 s, and device B has slightly larger negative shift than device A. Device B achieves negative shift of V_{TH}, while device A has a small positive shift of V_{TH} under PBS as shown in Fig. 5(b) and (e). The negative shift of V_{TH} under PBS attributes to doubly-ionized oxygen vacancy, ionized hydrogen and so on. On the contrary, the electron trapping results in positive shift of V_{TH} [37-40]. Obviously, donor-like defects in device B overwhelm electron trapping due to more V_O defects resulting from RF magnetron sputtering. The transfer process between ALD and RF magnetron sputtering steps also introduces more absorption of moisture in the air diffusing in

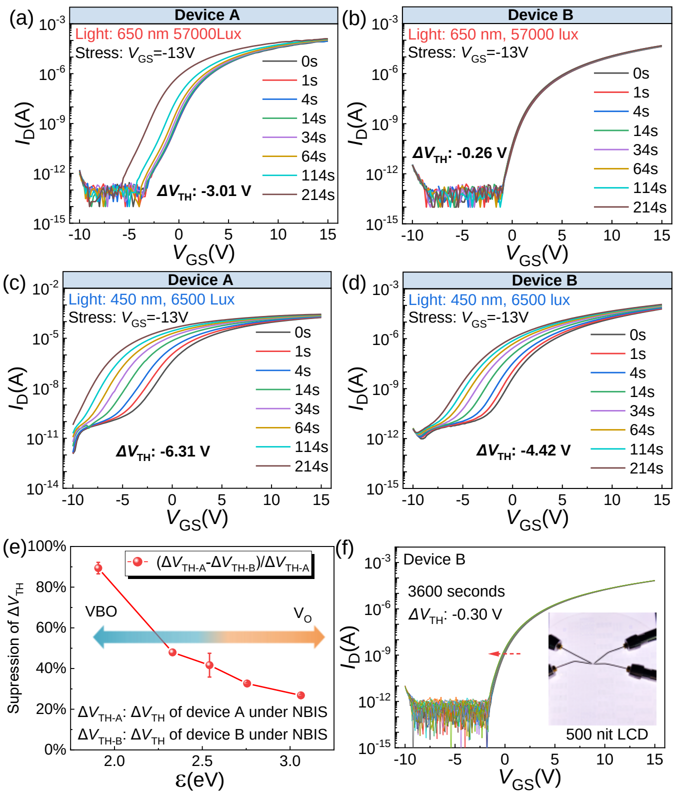

Fig. 6. The I_D-V_G of (a) device A, (b) device B under NBIS (650 nm laser of 57000 Lux, V_{GS}=-13 V, V_{DS}=0 V) for 214 s. The I_D-V_G of (c) device A, (d) device B under NBIS (450 nm laser of 6500 Lux, V_{GS}=-13 V, V_{DS}=0 V) for 214 s. (e) The suppression percent in ΔV_{TH} of device C relative to device A under laser of 650 nm (1.90 eV), 532 nm (2.33 eV), 488 nm (2.54 eV), 450 nm (2.75 eV) and 405 nm (3.06 eV) with V_{GS}=-13 V, V_{DS}=0 V for 214 s. (f) The I_D-V_G of device B under NBIS (back-light LCD of 500 nit, V_{GS}=-5 V, V_{DS}=0 V) for 3600 s.

ZnO, leading to more interstitial hydrogen related defects, which will exacerbate the negative shift of device under PBS. For the same reason, device A still shows better stability with small positive ΔV_{TH} than device B with negative ΔV_{TH} under PBIS. These results once again explain that device B with HBL has better stability under NBIS with more defects at interface and in channel. The enlarged VBO indeed largely suppresses the ΔV_{TH} under NBIS.

To better understand the roles of VBO and oxygen vacancy in degradation of TFTs under NBIS, the extreme high brightness lasers with different wavelengths are also employed to irradiate on device A and B. Fig. 6(a) and (b) show the transfer characteristics of device A and B under stress of V_{GS}=-13 V, V_{DS}=0 V for 214 s with red laser (650 nm, 57000 lux). The ΔV_{TH} of device B is -0.26 V, which is far less than -3.01 V of device A. The main reason is that the photon energy of 650 nm laser (1.90 eV) cannot excite holes in channel's valence band to cross barrier of VBO between ZnO and SiO_2. For device A, holes in channel can be easily excited by photon energy of 1.90 eV to enter Al_2O_3 due to its low VBO of 1.72 eV as shown in Fig. 3(d). Meanwhile, oxygen vacancies in channels are hardly ionized under this small photon energy. When a shorter wavelength of laser (450 nm, 2.73 eV, 6500 lux) is used in NBIS, as illustrated in Fig. 6(c) and (d), the ΔV_{TH} of device B is -4.42 V, close to -6.31 V of device A, as expected. Despite the low photon energy under VBO, device B still has a considerable negative ΔV_{TH}. It reveals that the oxygen vacancy related defects in channels have been ionized by the larger photo energy. The localized tail states also affect the real value of VBO, resulting in larger negative threshold voltage shift under gradual increasing photo energy. Moreover, excited by this short-wave laser, the off-current has an obvious increase. The main reason is that the electrons in valence band or trapped in forbidden band jump into conduction band after absorption of high photon energy. Three lasers of other wavelengths are also illuminated on devices with V_{GS}=-13 V, V_{DS}=0 V. The ΔV_{TH} of device A and B are -5.76 V, -2.05 V under green laser (532 nm, 311440 lux), and -5.57 V, -2.59 V under cyan laser (488 nm, 3400 lux), -5.93 V, -4.22 V under purple laser (405 nm, 650 lux), respectively. Owing to different power of the lasers, the relative suppression ratio is adopted in Fig. 6(e) to represent the improvement in ΔV_{TH} of device B compared with control sample device A, and the computational formula is described in the inset of Fig. 6(e), i.e. the better effect of suppression in ΔV_{TH}, the larger percentage described in ordinate. It can be found that the ΔV_{TH} of device B approaches that of device A gradually, when the light wavelength decreases or the photon energy increases. The case once again proves that the oxygen vacancy and the VBO between GI/channel codetermine the ΔV_{TH} of devices under NBIS from another perspective. When the photon energy is too low to excite the deep oxygen vacancy, VBO will in a great measure determine the degradation of TFTs under NBIS. While the photon energy approaches and exceeds the energy difference of oxygen vacancy and conduction band, the ionization of oxygen vacancy will gradually dominate ΔV_{TH} in degradation of device under NBIS.

Finally, device B is evaluated under the light of actual working environment as shown in Fig. 6(f), and the devices fabricated on glass in inset demonstrate a high degree of transparency. The device is measured on a 500-nit LCD back light panel for 3600 s, and exhibits the ΔV_{TH} of -0.3 V under V_{GS}=-5 V, V_{DS}=0 V. Generally, the luminance value of AMOLED/LCD screens in smartphones and displays is usually set at 250 nit that is entirely enough in most usage scenarios. Therefore, device B with HBL has potential to be used in transparent displays in future without sacrifice of transparency to suppress the NBIS issues of ZnO TFTs.

IV. Conclusion

In this work, the novel explanation of co-effect of valence band offset and oxygen vacancy on the ΔV_{TH} of ZnO devices under NBIS is investigated systematically. ZnO TFTs with HBL of SiO_2 are fabricated and evaluated under NBIS showing SiO_2 is an effective holes-blocking layer with a large VBO up to 3.08 eV relative to ZnO. A 500-nit LCD backlight is also used to simulate the working environment of TFTs in the display screen, and only -0.3V threshold voltage shift is tested under 3600 s. The result shows that device with HBL has better stability under NBIS without sacrifice of transparency and should be used in future study.

Acknowledgment

The authors gratefully acknowledge the Micro/Nano Fabrication Center and International Research Center for Information Science and Electronic Engineering, International Campus, Zhejiang University for support on fabrication and test. The authors also thank the ZJU Micro-nano Fabrication Center, ZJU State Key Laboratory of Silicon Materials and Jin Research Group, Zhejiang University for support on fabrication equipment, material characterization.

REFERENCES

[1] M. Tada, K. Mochizuki, T. Tsunashima, H. Tanaka, T. Ito, H. Watakabe, A. Hanada, R. Kimura, and Y. Ishii, "12-1: An Advanced LTPS TFT-LCD using Top-Gate Oxide TFT in Pixel," *SID Symposium Digest of Technical Papers*, vol. 49, no. 1, pp. 117-120, May. 2018, doi: 10.1002/sdtp.12497.

[2] H. Watakabe, T. Jinnai, I. Suzumura, A. Hanada, R. Onodera, M. Tada, K. Mochizuki, H. Tanaka, and T. Ito, "39-2: Development of Advanced LTPS TFT Technology for Low Power Consumption and Narrow Border LCDs," *SID Symposium Digest of Technical Papers*, vol. 50, no. 1, pp. 541-544, Jun. 2019, doi: 10.1002/sdtp.12977.

[3] T.-K. Chang, C.-W. Lin, and S. Chang, "39-3: Invited Paper: LTPO TFT Technology for AMOLEDs†," *SID Symposium Digest of Technical Papers*, vol. 50, no. 1, pp. 545-548, Jun. 2019, doi: 10.1002/sdtp.12978.

[4] R. Hoffman, B. J. Norris, and J. Wager, "ZnO-based transparent thin-film transistors," *Appl. Phys. Lett.*, vol. 82, Jan. 2003, doi: 10.1063/1.1542677.

[5] H. Oh, S.-H. K. Park, M. K. Ryu, C.-S. Hwang, S. Yang, and O. S. Kwon, "Improved Stability of Atomic Layer Deposited ZnO Thin Film Transistor by Intercycle Oxidation," *ETRI Journal*, vol. 34, no. 2, pp. 280-283, Apr. 2012, doi: 10.4218/etrij.12.0211.0186.

[6] W. Zhao, L. Han, N. Zhang, X. Zhang, S. Dong, Y. Liu, and Z. Ye, "High-Gain Transparent Inverters Based on Deuterated ZnO TFTs Fabricated by Atomic Layer Deposition," *IEEE Electron Device Lett.*, vol. 41, no. 10, pp. 1508-1511, Oct. 2020, doi: 10.1109/LED.2020.3018443.

[7] Z. Ye, M. Wong, M. Ng, and J. K. Luo, "High stability fluorinated zinc oxide thin film transistor and its application on high precision active-matrix touch panel," in *2013 IEEE International Electron Devices Meeting*, 9-11 Dec. 2013, pp. 27.2.1-27.2.4, doi: 10.1109/IEDM.2013.6724702.

[8] Z. Ye, H. Xu, T. Liu, N. Liu, Y. Wang, N. Zhang, and Y. Liu, "Highly Stable Atomic Layer Deposited Zinc Oxide Thin-Film Transistors Incorporating Triple O_2 Annealing," *IEEE Transactions on Electron Devices*, vol. 64, no. 10, pp. 4114-4122, Oct. 2017, doi: 10.1109/TED.2017.2737552.

[9] K. H. Ji, J.-I. Kim, H. Y. Jung, S. Y. Park, R. Choi, Y. G. Mo, and J. K. Jeong, "Comprehensive studies of the degradation mechanism in amorphous InGaZnO transistors by the negative bias illumination stress," *Microelectron. Eng.*, vol. 88, no. 7, pp. 1412-1416, Jul. 2011, doi: 10.1016/j.mee.2011.03.069.

[10] Y. Tu, I. Lu, H. Chen, W. Su, Y. Hung, K. Zhou, Y. Zheng, L. Sun, Y. Shih, J. Chen, C. Lien, H. Huang, C. Lien, and T. Chang, "Improving a-InGaZnO TFTs Reliability by Optimizing Electrode Capping Structure Under Negative Bias Illumination Stress," *IEEE Electron Device Lett.*, vol. 41, no. 8, pp. 1221-1224, Aug. 2020, doi: 10.1109/LED.2020.3006487.

[11] J. S. Park, T. S. Kim, K. S. Son, J. S. Jung, K. Lee, J. Kwon, B. Koo, and S. Lee, "Influence of Illumination on the Negative-Bias Stability of Transparent Hafnium–Indium–Zinc Oxide Thin-Film Transistors," *IEEE Electron Device Lett.*, vol. 31, no. 5, pp. 440-442, May. 2010, doi: 10.1109/LED.2010.2043050.

[12] H. Kim, K. Im, J. Park, T. Khim, H. Hwang, S. Kim, S. Lee, M. Song, P. Choi, J. Song, and B. Choi, "The Effects of Valence Band Offset on Threshold Voltage Shift in a-InGaZnO TFTs Under Negative Bias Illumination Stress," *IEEE Electron Device Lett.*, vol. 41, no. 5, pp. 737-740, May. 2020, doi: 10.1109/LED.2020.2981176.

[13] K. H. Ji, J.-I. Kim, H. Y. Jung, S. Y. Park, R. Choi, U. K. Kim, C. S. Hwang, D. Lee, H. Hwang, and J. K. Jeong, "Effect of high-pressure oxygen annealing on negative bias illumination stress-induced instability of InGaZnO thin film transistors," *Appl. Phys. Lett.*, vol. 98, no. 10, p. 103509, Mar. 2011, doi: 10.1063/1.3564882.

[14] P. Migliorato, M. Delwar Hossain Chowdhury, J. Gwang Um, M. Seok, and J. Jang, "Light/negative bias stress instabilities in indium gallium zinc oxide thin film transistors explained by creation of a double donor," *Appl. Phys. Lett.*, vol. 101, no. 12, p. 123502, Sept. 2012, doi: 10.1063/1.4752238.

[15] C. Deng, L. Lan, P. He, Y. Li, X. Li, S. Chen, and J. Peng, "Effect of Bandgap Widening on Negative-Bias Illumination Stress Stability of Oxide Thin-Film Transistors," *IEEE Transactions on Electron Devices*, vol. 68, no. 9, pp. 4450-4454, Jul. 2021, doi: 10.1109/TED.2021.3095135.

[16] J. Kim, J. Bang, N. Nakamura, and H. Hosono, "Ultra-wide bandgap amorphous oxide semiconductors for NBIS-free thin-film transistors," *APL Materials*, vol. 7, no. 2, p. 022501, Feb. 2019, doi: 10.1063/1.5053762.

[17] H. Oh, S.-M. Yoon, M. K. Ryu, C.-S. Hwang, S. Yang, and S.-H. K. Park, "Photon-accelerated negative bias instability involving subgap states creation in amorphous In–Ga–Zn–O thin film transistor," *Appl. Phys. Lett.*, vol. 97, no. 18, p. 183502, Nov. 2010, doi: 10.1063/1.3510471.

[18] S. Li, M. Wang, D. Zhang, H. Wang, and Q. Shan, "A Unified Degradation Model of a-InGaZnO TFTs Under Negative Gate Bias With or Without an Illumination," *IEEE Journal of the Electron Devices Society*, vol. 7, pp. 1063-1071, Oct. 2019, doi: 10.1109/JEDS.2019.2946383.

[19] S. Yang, D.-H. Cho, M. K. Ryu, S.-H. K. Park, C.-S. Hwang, J. Jang, and J. K. Jeong, "Improvement in the photon-induced bias stability of Al–Sn–Zn–In–O thin film transistors by adopting AlOx passivation layer," *Appl. Phys. Lett.*, vol. 96, no. 21, p. 213511, May. 2010, doi: 10.1063/1.3432445.

[20] C. W. Kuo, T. C. Chang, Y. C. Chien, Y. L. Tsai, H. Y. Tu, Y. C. Tsao, Y. T. Chien, H. C. Chen, J. J. Chen, T. M. Tsai, and S. M. Sze, "On the Optimization of Performance and Reliability in a-InGaZnO Thin-Film Transistors by Versatile Light Shielding Design," *IEEE Transactions on Electron Devices*, vol. 68, no. 4, pp. 1654-1658, Apr. 2021, doi: 10.1109/TED.2021.3058195.

[21] S. Lee, M. Mativenga, and J. Jang, "Removal of Negative-Bias-Illumination-Stress Instability in Amorphous-InGaZnO Thin-Film Transistors by Top-Gate Offset Structure," *IEEE Electron Device Lett.*, vol. 35, no. 9, pp. 930-932, Sept. 2014, doi: 10.1109/LED.2014.2333014.

[22] E. G. Lee, J. Park, S. Lee, H. Na, N. Cho, C. Im, Y. H. Cho, and Y. S. Kim, "Oxygen Radical Control via Atmospheric Pressure Plasma Treatment for Highly Stable IGZO Thin-Film Transistors," *IEEE Transactions on Electron Devices*, vol. 67, no. 8, pp. 3135-3140, Aug. 2020, doi: 10.1109/TED.2020.3000736.

[23] E. Kim, W. J. Jang, W. Kim, J. Park, M. K. Lee, S. K. Park, and K. C. Choi, "Suppressed Instability of a-IGZO Thin-Film Transistors Under Negative Bias Illumination Stress Using the Distributed Bragg Reflectors," *IEEE Trans. Electron Devices*, vol. 63, no. 3, pp. 1066-1071, Mar. 2016, doi: 10.1109/TED.2015.2513414.

[24] L. Lu, Z. Xia, J. Li, Z. Feng, S. Wang, H. S. Kwok, and M. Wong, "A Comparative Study on Fluorination and Oxidation of Indium–Gallium–Zinc Oxide Thin-Film Transistors," *IEEE Electron Device Lett.*, vol. 39, no. 2, pp. 196-199, Feb. 2018, doi: 10.1109/LED.2017.2781700.

[25] S. Deng, S.-C. Dong, R. Chen, W. Zhong, G. Li, M. Zhang, F. S. Y. Yeung, M. Wong, and H.-S. Kwok, "A cost-effective fluorination method for enhancing the performance of metal oxide thin-film transistors," *Journal of the Society for Information Display*, vol. 29, no. 5, pp. 318-327, May. 2021, doi: 10.1002/jsid.1013.

[26] M. Furuta, J. Jiang, G. Tatsuoka, and D. Wang, "(Invited) Doping and Defect Passivation in In-Ga-Zn-O by Fluorine," *ECS Trans.*, vol. 67, no. 1, pp. 41-49, May. 2015, doi: 10.1149/06701.0041ecst.

[27] S. Y. Park, J. H. Song, C. K. Lee, B. G. Son, C. K. Lee, H. J. Kim, R. Choi, Y. J. Choi, U. K. Kim, C. S. Hwang, H. J. Kim, and J. K. Jeong, "Improvement in Photo-Bias Stability of High-Mobility Indium Zinc Oxide Thin-Film Transistors by Oxygen High-Pressure Annealing," *IEEE Electron Device Lett.*, vol. 34, no. 7, pp. 894-896, Jul. 2013, doi: 10.1109/LED.2013.2259574.

[28] S. Yang, K. Hwan Ji, U. Ki Kim, C. Seong Hwang, S.-H. Ko Park, C.-S. Hwang, J. Jang, and J. Kyeong Jeong, "Suppression in the negative bias illumination instability of Zn-Sn-O transistor using oxygen plasma treatment," *Appl. Phys. Lett.*, vol. 99, no. 10, p. 102103, Sept. 2011, doi: 10.1063/1.3634053.

[29] D. Zhong, J. Li, C. Zhao, C. Huang, J. Zhang, X. Li, X. Jiang, and Z. Zhang, "Enhanced Electrical Performance and Negative Bias Illumination Stability of Solution-Processed InZnO Thin-Film Transistor by Boron Addition," *IEEE Transactions on Electron Devices*, vol. 65, no. 2, pp. 520-525, Feb. 2018, doi: 10.1109/TED.2017.2779743.

[30] J. K. Saha, A. Ali, R. N. Bukke, Y. G. Kim, M. M. Islam, and J. Jang, "Performance Improvement for Spray-Coated ZnO TFT by F Doping With Spray-Coated Zr–Al–O Gate Insulator," *IEEE Transactions on Electron Devices*, vol. 68, no. 3, pp. 1063-1069, Mar. 2021, doi: 10.1109/TED.2021.3051918.

[31] J. S. Jung, K.-H. Lee, K. S. Son, J. S. Park, T. S. Kim, J. H. Seo, J.-H. Jeon, M.-P. Hong, J.-Y. Kwon, B. Koo, and S. Lee, "The Effect of Passivation Layers on the Negative Bias Instability of Ga–In–Zn–O Thin Film Transistors under Illumination," *Electrochem. Solid-State Lett.*, vol. 13, no. 11, p. H376, Aug. 2010, doi: 10.1149/1.3481710.

[32] J. Park, N. D. Trung, Y. S. Kim, J. H. Kim, K. Park, and H.-S. Kim, "A study on the competition between bias-induced charge trapping and light-induced instability in In-Ga-Zn-O thin-film transistors," *J. Electroceram.*, vol. 36, no. 1, pp. 135-140, Jun. 2016, doi: 10.1007/s10832-016-0032-3.

[33] S. Yoon, Y. J. Tak, D. H. Yoon, U. H. Choi, J.-S. Park, B. D. Ahn, and H. J. Kim, "Study of Nitrogen High-Pressure Annealing on InGaZnO Thin-Film Transistors," *ACS Applied Materials & Interfaces*, vol. 6, no. 16, pp. 13496-13501, Aug. 2014, doi: 10.1021/am502571w.

[34] C.-Y. Jeong, I.-J. Park, I.-T. Cho, J.-H. Lee, E.-S. Cho, M. K. Ryu, S.-H. K. Park, S.-H. Song, and H.-I. Kwon, "Investigation of the Low-

Frequency Noise Behavior and Its Correlation with the Subgap Density of States and Bias-Induced Instabilities in Amorphous InGaZnO Thin-Film Transistors with Various Oxygen Flow Rates," *Japanese Journal of Applied Physics,* vol. 51, p. 100206, Oct. 2012, doi: 10.1143/jjap.51.100206.

[35] S. Kim, Y. Jeon, J. H. Lee, B. D. Ahn, S. Y. Park, J. H. Park, J. H. Kim, J. Park, D. M. Kim, and D. H. Kim, "Relation Between Low-Frequency Noise and Subgap Density of States in Amorphous InGaZnO Thin-Film Transistors," *IEEE Electron Device Lett.,* vol. 31, no. 11, pp. 1236-1238, Sept. 2010, doi: 10.1109/LED.2010.2061216.

[36] Z. Ye, Y. Yuan, H. Xu, Y. Liu, J. Luo, and M. Wong, "Mechanism and Origin of Hysteresis in Oxide Thin-Film Transistor and Its Application on 3-D Nonvolatile Memory," *IEEE Transactions on Electron Devices,* vol. 64, no. 2, pp. 438-446, Feb. 2017, doi: 10.1109/TED.2016.2641476.

[37] Z. Jiang, M. Zhang, S. Deng, Y. Yang, M. Wong, and H. S. Kwok, "Evaluation of Positive-Bias-Stress-Induced Degradation in InSnZnO Thin-Film Transistors by Low Frequency Noise Measurement," *IEEE Electron Device Lett.,* vol. 43, no. 6, pp. 886-889, Jun. 2022, doi: 10.1109/LED.2022.3165558.

[38] J. Li, H. Peng, H. Yang, X. Zhou, L. Lu, and S. Zhang, "Abnormal Bias Instabilities Induced by Lateral H_2O Diffusion into Top-Gate Insulator of a-InGaZnO Thin-Film Transistors," *IEEE Journal of the Electron Devices Society,* vol. 10, pp. 341-345, Apr. 2022, doi: 10.1109/JEDS.2022.3167963.

[39] Y. Yang, D. Zhang, M. Wang, L. Lu, and M. Wong, "Suppressed Degradation of Elevated-Metal Metal–Oxide Thin-Film Transistors Under Bipolar Gate Pulse Stress," *IEEE Electron Device Lett.,* vol. 39, no. 5, pp. 707-710, May. 2018, doi: 10.1109/LED.2018.2821366.

[40] S. Jin, T. Kim, Y. Seol, M. Mativenga, and J. Jang, "Reduction of Positive-Bias-Stress Effects in Bulk-Accumulation Amorphous-InGaZnO TFTs," *IEEE Electron Device Lett.,* vol. 35, no. 5, pp. 560-562, May. 2014, doi: 10.1109/LED.2014.2311172.